Journal of Electroceramics
https://doi.org/10.1007/s10832-018-0143-0

Structural and electrical transport properties of Pr-doped $SrTi_{0.93}Co_{0.07}O_{3-\delta}$ a novel SOEC fuel electrode materials

B. Kamecki[1] · T. Miruszewski[1] · J. Karczewski[1]

Received: 21 November 2017 / Accepted: 28 May 2018

Abstract
Solid Oxide Electrolyzer Cells (SOECs) are very promising electrochemical devices for the production of syngas (H_2/CO) by H_2O and CO_2 co-electrolysis. The structure, microstructure and electrical properties of the fuel electrode material play a crucial role in the performance of the whole cell and efficiency of electrocatalytic reduction of steam into hydrogen. In the present work, a novel Co and Pr co-doped $SrTiO_{3-\delta}$ material attracted attention as a potential fuel electrode for SOFC/SOEC. Materials with different praseodymium content were prepared by a solid-state reaction process. XRD confirmed cubic perovskite structure in all obtained samples. SEM results showed porosity in doped materials and EDX proved ABO_3 stoichiometry. TEC values were about 1.17–1.26•10^{-5} K^{-1} very close to the YSZ electrolyte value. XPS studies turn out that a praseodymium can be multivalent and exist on mixed +3 and + 4 oxidation state. Electrical conductivity of samples was measured by DC 4-wire method in range of 100-800 °C. Highest value of total conductivity was achieved for $Sr_{0.7}Pr_{0.3}Ti_{0.93}Co_{0.07}O_{3-\delta}$ and reached 23.7 S·cm^{-1}. The obtained results were discussed and analyzed in term of defect chemistry.

Keywords MIEC · SOFC · SOEC · Strontium titanate · Electrical conductivity · Perovskites

1 Introduction

At the current stage of energy sources development, the production of energy from renewables is one of the conceptions to solve the growing energy demand problem. The energy from renewable sources is usually supplied discontinuously, so it is required to be storaged. The very interesting concept is to produce a pure hydrogen or syngas (H_2 + CO) by using the electrochemical devises such as Solid Oxide Electrolysis Cells (SOECs). The SOECs devices are now very widely studied devices, because of its high efficiency process of changing electricity to fuel [1].

One of the main drawback making difficult to spread the solid oxide electrolysis technology is rapid degradation of the systems. The understanding of degradation processes of fuel electrode is crucial for improve their electrochemical properties. Particular attention should be paid to the processes taking place in extreme conditions - high current density and high concentration of steam and carbon dioxide. For state of the art fuel electrode material Ni-YSZ cermet, it has been reported that under high current density and reducing atmosphere a fast degradation process occurs, *i.a.* an interruption in Ni-Ni percolation paths, which can replace a Triple Phase Boundary (TPB) points away from the electrolyte/electrode interface [2] or also a formation process of nanozirconia and nickel hydroxide [3]. All these mechanism significantly decrease the total efficiency of SOEC. Thus a new alternative, cathode materials should be found and widely investigated. Some perovskite type materials were investigated as a potential candidates: *i.a.* $La_{0.25}Sr_{0.75}Cr_{0.5}Mn_{0.4}Sc_{0.1}O_3$ (LSCMS) [1], $(La_{0.2}Sr_{0.8})_{0.9}Ti_{0.9}Fe_{0.1}O_3$ (LSTFO) [4] or Sr_2FeNbO_3 [5].

The microstructure of the new cathode material on its electrical properties has a great influence on performance and stability of the cell producing synthesis gas, operating under heavy load [1, 4]. Doped strontium titanate $SrTiO_3$ ceramics (STO) have been attracting attention due to its unique properties in terms of use in electrochemical devices like SOFC/SOEC. The counter hopping transport of oxygen ions via an oxygen vacancies and simultaneous electron hopping in the $Ti^{3+} - O^{2-}$ - Ti^{4+} network due to the covalent overlapping of the Ti-3d and O-2p orbitals makes a STO ceramics a mixed ionic-electronic conductor (MIEC) [6–8]. Non-modified $SrTiO_3$ has insulating properties, but additional doping

✉ B. Kamecki
bartosz.kamecki@pg.edu.pl

[1] Faculty of Applied Physics and Mathematics, Solid State Physics Department, Gdańsk University of Technology, ul. G. Narutowicza 11/12, 80-233 Gdańsk, Poland

Published online: 07 June 2018

process or thermal treatment at low pO_2 conditions can change its electrical properties [9]. Its conductivity increases significantly at low oxygen partial pressure according to a change in the titanium valence from Ti^{4+} to Ti^{3+}. The conductivity mechanism in STO materials is related to the double-exchange mechanism. In STO, donor dopant in such materials provides to the formation of quasi-free conduction electrons and by the formation of cation strontium vacancies. On the other hand, the addition of acceptor dopants in the system leads to creation of either doubly ionized oxygen vacancies or electron holes. Donor substituted strontium titanate exhibits suitable electrical conductivity and excellent structural stability for SOFC/SOEC application. For example, for yttrium doped $SrTiO_3$ reduced in H_2 has been reported very high electrical conductivity in comparison to other rare earth substitutes [10]. On the other hand acceptor doped $Sr(Ti,Fe)O_3$ has shown as an oxygen ions conductor properties [11–15]. Recent theoretical calculations and experimental results shown that donor and acceptor co-doping of strontium titanate into the two different sublattice (Sr and Ti) can induce a mixed ionic-electronic conductivity (MIEC) [16, 17].

2 Defect chemistry of Pr, co-doped strontium titanate

The mixed ionic and electronic conductivity in materials is a crucial phenomenon which allows applying material to electrochemical devices. One way to improve the partial conductivities is a co-doping of perovskite materials. Both donors (such as yttrium, or lanthanum) and acceptors (such as cobalt, iron or aluminum) in $SrTiO_3$ can modify electronic and ionic conductivity. However, the final electrical properties caused by co-doping can be sometimes more complex. In a donor and acceptor co-doped $SrTiO_3$ material, the total conductivity is a result of the interaction between the electronic defects like an electrons or holes (depends on pO_2) generated by the donor and the acceptor. For example, in co-doped $SrTiO_3$, part of the electrons generated by the donor may be compensated by electron holes generated by the acceptor. Moreover, the oxygen vacancies created by the acceptor dopant can have an influence on electronic conduction mechanism. That is why sometimes the acceptor dopant into the donor doped $SrTiO_3$ can improve the ionic conductivity but decrease the electronic part. It was observed *i.a.* in Li et al. [18, 19] works. The optimal mixed conductivity can be obtained by the good choose of the dopant cations and moreover, by the optimal concentrations ratio between the donor and acceptor dopants.

It can be stated, that the defect chemistry of donor and acceptor doped is studied for nearly fifty years [9, 18–22]. However, the compensation mechanisms are not established completely. In case of donor and acceptor co-doped $SrTiO_3$, the compensation of donor and acceptor dopants strongly depends on the oxygen partial pressure (reducing or oxidizing atmospheres). In case of different atmosphere, the defect chemistry, and in consequence, the electrical properties may be quite different. In this assumption stoichiometric $SrTiO_3$ were doped by praseodymium and cobalt cations $Sr_{1-x}Pr_xTi_yCo_{1-y}O_3$. It should be mentioned here, that the praseodymium cation can exist in the structure in the different valence state – Pr^{2+}, Pr^{3+} and Pr^{4+}, so the praseodymium can substitute both Sr and Ti sublattice. The sublattice, where the praseodymium dopant will be incorporated strongly depends on its valence state and the pO_2. In this case the full electroneutrality (independent of pO_2) condition (ENC) can be presented as Eq. 1:

$$n + 2\left[V''_{Sr}\right] + 2\left[O''_i\right] + \left[Pr'_{Ti}\right] + \left[Co'_{Ti}\right] = p + 2\left[V^{\bullet\bullet}_O\right] + \left[Pr^{\bullet}_{Sr}\right] \quad (1)$$

where *n, p* denotes the electrons and hole, respectively. The $\left[V''_{Sr}\right]$ is a concentration of strontium vacancies and $\left[O''_i\right]$ denotes an interstitial oxygen. The trivalent Pr^{3+} praseodymium donor dopant concentration in the Sr^{2+} sublattice was denotes as a $\left[Pr^{\bullet}_{Sr}\right]$. In the equations described above, the another, neutral defects like a $\left[\mathrm{Pr}^{x}_{Sr}\right]$ and $\left[\mathrm{Pr}^{x}_{Ti}\right]$ was not mentioned. This defects can be occure when the Pr^{4+}cation will substitute the Ti^{4+} sublattice or Pr^{2+} substitute the Sr^{2+} sublattice. Because this type of dopant is isovalent, no electrical properties but only the structural properties change will be observed in the samples. It is assumed that the formation of a double charge defect (Pr^{2+} in place of Ti^{4+} or Pr^{4+} in place of $Sr^{2+)}$ is highly unlikely and negligible in these considerations. Introducing of Pr^{3+} donor dopant into the Sr^{2+} site affect the creating of quasi-free electron in the conduction band according to Eq. 2:

$$Pr_2O_3 \xrightarrow{SrTiO_3} 2Pr^{\bullet}_{Sr} + 2e' + 3O^x_O \quad (2)$$

In this case, the electronic conductivity of material should increase. However most commonly, the compensation process is quite more complex. Further, the Pr^{3+} praseodymium cation in the Ti^{4+} sublattice in Eq. 1 is denoted as $\left[Pr'_{Ti}\right]$. Then, this is an acceptor dopant. The Co^{3+} dopant in the Ti^{4+} sublattice is denoted as $\left[Co'_{Ti}\right]$. When the titanium cation is rather at Ti^{4+} state and then Co^{3+} ions can replace Ti^{4+} ions, which can be expressed in Eq. 3:

$$Co_2O_3 \xrightarrow{SrTiO_3} 2Co'_{Ti} + V^{\bullet\bullet}_O + 3O^x_O \quad (3)$$

As can be seen, the acceptor dopant is compensated by the oxygen vacancies. In this case, the ionic conductivity of $SrTiO_{3-\delta}$ should increase because of the increase of the oxygen vacancies. It was experimentally proved and reported *i.a.* by Li et al. [18] in La, Co co-doped $SrTiO_3$ ceramics.

As been mentioned, the compensation mechanism in doped $SrTiO_3$ strongly depends on the pO_2 parameter. At high oxygen partial pressures (under oxidation atmospheres) the electron holes $p = [h^{\bullet}]$ and strontium vacancies $\left[V''_{Sr}\right]$ are predominant defects. In this case, the electroneutrality condition can be presented as Eq. 4:

$$2\left[V''_{Sr}\right] + \left[Pr'_{Ti}\right] + \left[Co'_{Ti}\right] = p + 2\left[Pr^{\bullet}_{Sr}\right] \quad (4)$$

The concentration of oxygen vacancies and electrons are negligible in these pO_2 regimes. At high pO_2 the concentration of holes decrease when the amount of the Pr^{3+} in the Sr^{2+} sublattice increase. Thus, the conductivity of material should decreases with increasing concentration of $\left[Pr^{\bullet}_{Sr}\right]$ and increases with increasing concentration of $\left[Pr'_{Ti}\right]$. Observing the conductivity change as a function of the dopant concentration one should be able to determine the position of praseodymium in the structure.

The second type of compensation takes place at low oxygen partial pressures (very reducing conditions, i.a. H_2 atmosphere) and in this case no strontium vacancies are observed. The oxygen vacancies and electron holes are predominant. The electroneutrality condition for low pO_2 conditions can be described in Eq. 5.:

$$n + \left[Pr'_{Ti}\right] + \left[Co'_{Ti}\right] = 2\left[V^{\bullet\bullet}_{O}\right] + \left[Pr^{\bullet}_{Sr}\right] \quad (5)$$

$$n = \left[e'\right] = \left[Ti'_{Ti}\right] \quad (6)$$

At low pO_2, the substitution of Pr^{3+} in the Sr^{2+} sublattice introduce the trivalent titanium cations Ti^{3+} in the system. The electron from a donor is then localized in a Ti^{4+}/Ti^{3+} cations pair and the conduction mechanism is related to the small-polaron hopping between the Ti^{4+}/Ti^{3+} pair. It is also worthy to underline, that under reducing atmospheres the oxygen nonstoichiometry is also present in the system because of the incorporation of the oxygen atoms from the oxygen sublattice. Under this assumption, under low pO_2 the oxygen vacancies and dopants are compensated by the electrons localized in the Ti^{4+}/Ti^{3+} pair. The conductivity of material at low pO_2 should behave the opposite way than in case of high pO_2, increase when the concentration of the $\left[Pr^{\bullet}_{Sr}\right]$ increases and decreases with increasing the concentration of the $\left[Pr'_{Ti}\right]$.

In this work, a Co-doped strontium titanate samples $Sr_{1-x}Pr_xTi_{0.93}Co_{0.07}O_3$ with different amount of praseodymium dopant were investigated. The 7 mol% of Co acceptor dopant was chosen according to the previous literature reports [18]. The praseodymium is introduced to strontium titanate in order to improve the electrical conductivity and to stabilize the cubic perovskite structure at wide oxygen partial pressure range. The cobalt dopant as an acceptor dopant was chosen in order to improve the ionic partial conductivity and the catalytic activity of the material. The structural and electrical properties of sintered ceramics were investigated in regard to SOFC/SOEC application.

3 Experimental

The ceramic samples with nominal cation stoichiometry $Sr_{1-x}Pr_xTi_{0.93}Co_{0.07}O_{3-\delta}$ (x = 0, 0.1, 0.2 and 0.3) were prepared via conventional solid state synthesis method. In this paper, the abbreviations referring to the Pr content was used (for example $Sr_{0.90}Pr_{0.1}Ti_{0.93}Co_{0.07}O_{3-\delta}$, is labeled as 10% Pr). The precursor powders of $SrCO_3$ (Chempur, 99%), TiO_2 (BDH Prolabo, 99%), Pr_6O_{11} (Fluka 99,9%), Co_2O_3 (POCH 99,9%) were ground and mixed in agate mortar and uniaxially pressed into a pellets. In the first step, the samples were calcined at 1200 °C for 10 h in pure hydrogen atmosphere. Heating and cooling temperature rate was 5 °C per minute. After that, the ceramics were milled in the ball mill for 15 h in isopropanol with zirconia balls. In the next step, the powders were pressed into pellets and were sintered at 1400 °C under the same condition as before.

The structure and phase composition of samples were analyzed by the X-ray diffraction technique (XRD) using the Philips X'Pert Pro MPD with $CuK_{\alpha 1}$ $\lambda = 0.15406$ nm. For X-rays diffraction the ceramic samples were ground to powder in agate mortar. Unit cells parameters were determined using LeBail refinement in *FullProf* software. The morphology of obtained samples was investigated by scanning electron microscopy (FEI Quanta FEG 250) with ET (Everhart-Thornley) secondary electron detector. Beam accelerating voltage was kept at 10 kV. For elemental analysis the Energy Dispersive X-ray Spectroscopy was performed by EDAX Genesis APEX 2i with ApolloX SDD spectrometer. X-ray Photoelectron Spectroscopy (XPS) was conducted using a Omicron Nanotechnology equipment with an unmonochromated MgK_{α} (1253.6 eV) radiation, source power of 15 kV and emission current 20 mA. A small amount of silver was applied on the surface for obtain a standardization in the binding energy by analyzing of the $Ag3d_{5/2}$ transitions at the energy of 368.2 eV. Deconvolution of recorded XPS spectra was conducted in CasaXPS software. Relative length changes $\Delta l/l$ during heating process was detected using a Netsch DIL 402 PC/4 dilatometer at a temperature range from 25 °C to 800 °C.

In order to analyze the electrical properties of the fabricated ceramics, the total electrical conductivity was measured by the conventional DC 4-wire method by the Keysight 3490A multimeter. The measurements were performed in a temperature range of 100–800 °C at pure hydrogen atmosphere and in air atmosphere (in typical SOEC cathode/anode operating conditions). The measurements with a four silver electrodes were performed at constant heating and cooling rates 5 °C/min. For one chosen $Sr_{1-x}Pr_xTi_{0.93}Co_{0.07}O_{3-\delta}$ sample the

measurements were taken after holding samples at each temperature for 1200s in order to make sure that during dynamic measurements the thermal equilibrium condition was reached in all analyzed samples. In both measurements identical results were obtained, therefore further measurements were made using the dynamic method.

4 Results and discussion

4.1 Structural properties

In order to determine the crystal structure of the analyzed $Sr_{1-x}Pr_xTi_{0.93}Co_{0.07}O_{3-\delta}$ compounds, the X-ray diffraction (XRD) measurements were performed. The XRD patterns are presented in Fig. 1. As it can be noticed, in all samples containing praseodymium besides of the cubic perovskite (Pr,Sr)(Ti,Co)O_3 phase with a space group *Pm-3 m* the small amounts of Pr_2O_3 phase was observed. Moreover, the amount of the secondary phase decreases with an increase Pr donor dopant concentration. This may indicate that the high concentration of Pr dopant in the structure is favorable for obtain a single phase material at 1400 °C. In order to investigate the influence of the praseodymium dopant on the lattice parameter and on the stability of a perovskite structure, the LeBail analysis was performed. The results are summarized in Table 1 and also presented in Fig. 2. As can be seen, the lattice parameter of obtained materials changes in a function of Pr donor dopant concentration. This lattice parameter growth can be explained in reference to the defect chemistry of donor-doped $SrTiO_3$. As been mentioned in the introduction section, there are several possibilities of Pr doping process in the

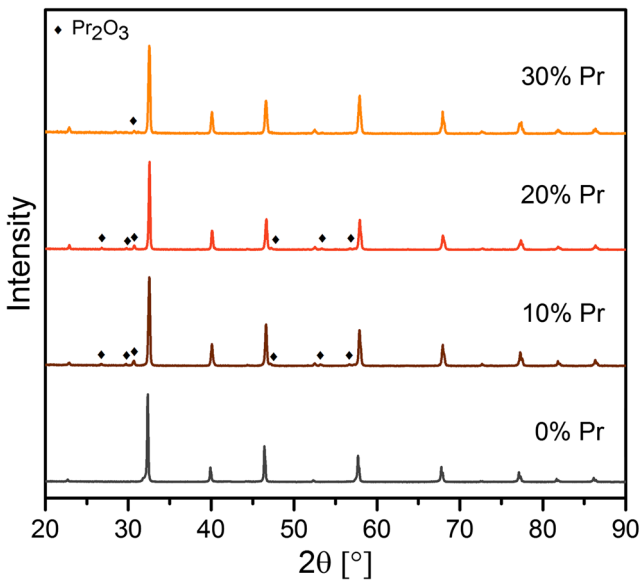

Fig. 1 XRD patterns for analyzed samples synthesized at 1400 °C for 10 h in H_2. The second phase Pr_2O_3 is marked in the patterns

Table 1 LeBail refinement results for $Sr_{1-x}Pr_xTi_{0.93}Co_{0.07}O_{3-\delta}$ samples sintered at 1400 °C for 10 h in H_2

Pr dopant concentration	Lattice parameters		Chi square χ^2
	a (Å)	*V* (Å^3)	
0	3.90509(7)	59.552(2)	3.08
0.1	3.90592(7)	59.590(2)	2.60
0.2	3.90683(6)	59.631(6)	2.59
0.3	3.90826(8)	59.697(2)	1.88

$SrTiO_3$ structure. The Pr^{2+} and Pr^{3+} cation can substitutes a Sr^{2+} sublattice and a Pr^{3+} and Pr^{4+} cation can be incorporated into a Ti^{4+}/Ti^{3+} sublattice. As was shown in Eq. 1 the concentration of Ti^{3+} is proportional to the donor and oxygen vacancies concentration. The ionic radius of trivalent Ti^{3+} cations (0.670 Å) is higher than a radius of Ti^{4+} (0.605 Å). Thus, when the concentration of Pr^{3+} dopant (and simultaneously Ti^{3+}) increases, the lattice parameter also should increase. This hypothesis well agrees with the experimental results and indicate that a Pr^{3+} cation substitutes a strontium perovskite sublattice (see Table 1). On the other hand, under the assumption that a tetravalent praseodymium cation (0.96 Å) substitutes a Ti^{4+}/Ti^{3+} sublattice (0.605/0.670 Å), the lattice parameter should increase. This result also agrees with behavior observed in Fig. 2. If both Pr^{3+} and Pr^{4+} cations will be assumed as a dopant only into a Sr^{2+} site (1.44 Å), the lattice parameter should decrease in a function of Pr dopant concentration what is contradicted with experimental results shown in Fig. 2.

Figures 3 and 4 present SEM and EDX results, respectively. Besides that, Table 2 summarize calculated amounts of atoms from EDX spectra for each sample. Fig. 3(a) shows fractured surface of the reference sample (0% Pr). An EDX

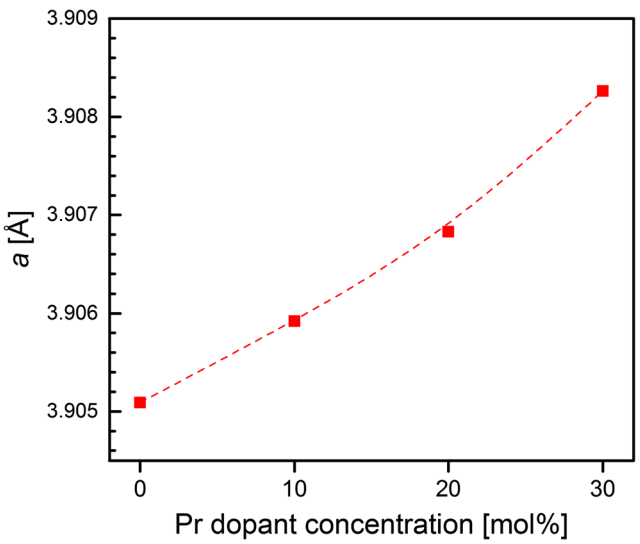

Fig. 2 Lattice parameter in a function of Pr donor dopant concentration in samples sintered in H_2 atmosphere at 1400 °C for 10 h

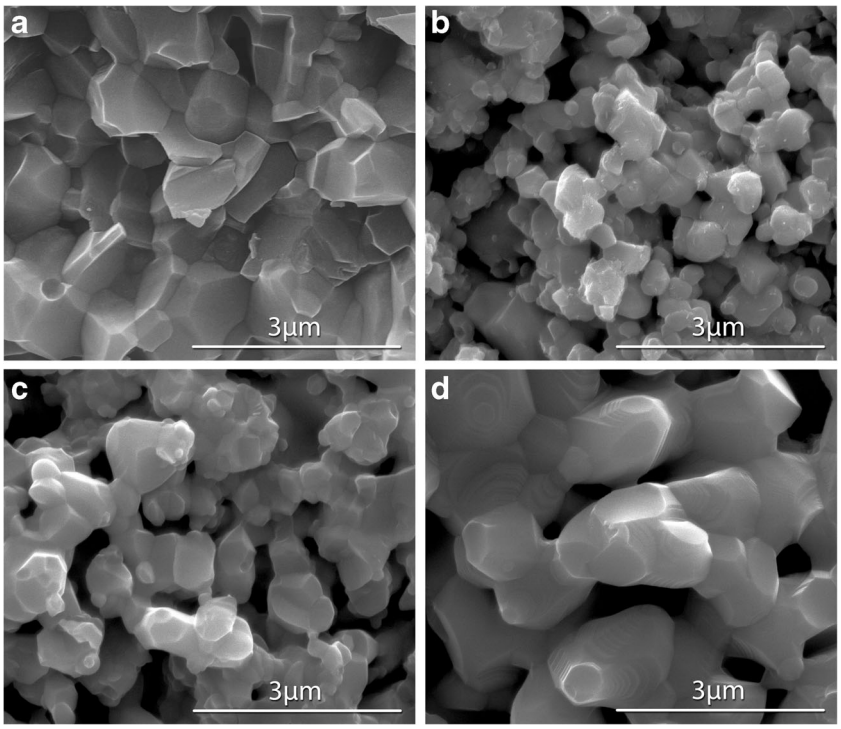

Fig. 3 Cross-sections SEM images of ceramics with a Pr dopant content of (**a**) 0%, (**b**) 10%, (**c**) 20%, (**d**)30%

studies on polished surface of this sample (Fig. 5) showed white spherical precipitations identificated as a cobalt in a metallic form. That small amount of metallic cobalt occurs as sintering aids and lead to the enhancement of the performance of densifying mechanism. In this case cobalt caused lowering sintering temperature and the higher density of sample can be observed [23]. Probably, cobalt cannot fully substitute the titanium in the structure without a presence of praseodymium donor dopant. It is worthy to underline, that cobalt in metallic form was not observed in the other investigated samples. It can be a reason, why a dense structure was not observed in the samples containing praseodymium.

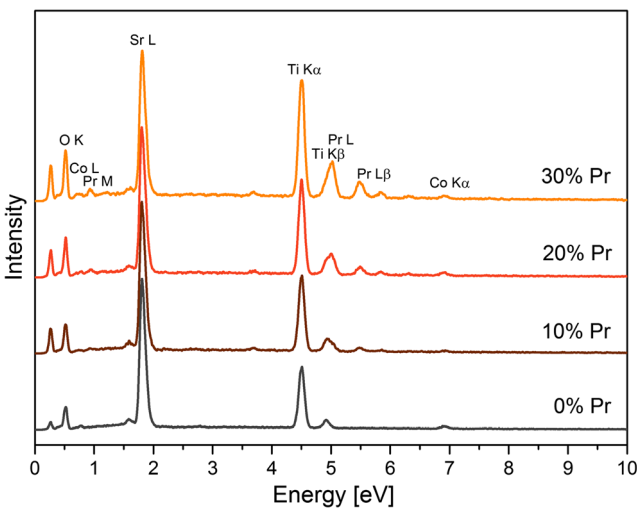

Fig. 4 EDX results of materials containing 0%, 10%, 20 and 30% of praseodymium dopant

Figure 3(b, c, d) represent the cross-section of the ceramics doped by praseodymium (10%, 20 and 30% respectively). All doped materials were porous and had the spherical shape grains. With increase of praseodymium dopant concentration, the grains are bigger. The average grain size varies from 500 nm to slightly over 1 μm. In sample with 10% of Pr dopant a small amount of white precipitates on the granules surface can be noticed.

The EDX studies confirmed that it is a praseodymium oxide Pr_2O_3. This result is strongly correlated with a XRD results for this sample (Fig. 1). Moreover, the EDX studies also confirmed that characteristic stoichiometry of perovskite structure in all compounds was present. The total porosity of investigated samples was also measured by the Archimedes method. The porosity values were about 30% for all samples with praseodymium what is compatible with SEM analysis.

X-ray Photoelectron Spectroscopy (XPS) is a surface sensitive technique. Thus in orders to properly perform the experiment, the powders of samples were used in the experiment. In case of the powder form of investigated samples, it is allowed to determine the oxidation states of praseodymium and titanium cations in crystallites from the bulk of the sample, not only from the surface. The analysis was conducted by deconvolution of praseodymium and titanium XPS spectra. The measurements were performed for each of synthesized samples. The comparison of titanium 2p core level was shown in Fig. 6. The shape of the spectrum was the same as in the examples that can be found in previous literature characterizing the strontium titanate compound. In both cases, titanium doublets with binding energy of 464.2 eV and 458.5 eV are

Table 2 Amounts of elements calculated from EDX spectra

sample	O teor	O (± 3%)	Sr teor	Sr (± 0,5%)	Ti teor	Ti (± 0,5%)	Pr teor	Pr (± 0,5%)	Co teor	Co (± 0,5%)
0% Pr	60	59	20	19,5	18,5	20	0		1,5	1,5
10% Pr		58,5	18	18		21	2	2		1
20% Pr		57,5	16	16		21	4	4		1,5
30% Pr		58	14	13,5		21,5	6	6		1

present. The binding energy values correspond respectively to the $Ti2p_{1/2}$ and $Ti2p_{3/2}$ band, characteristic for Ti^{4+} [24, 25]. An additional doublet at a lower binding energy regime, typically assigned to Ti^{3+}, was also detected. For each samples, the second doublet was shifted towards to the lower binding energies by about 2.2 eV. It is shown that the praseodymium dopant makes a partial reduction of a titanium cation from Ti^{+4} to Ti^{+3}. This is in agreement with a defect chemistry of this type of dopant in $SrTiO_3$ (Eqs.5 and 6). The higher concentration of praseodymium in the structure affects the increase of the trivalent titanium.

Figure 7 presents an example of the XPS spectra for praseodymium core $3d_{5/2}$. The figure shows results for material with 30 mol% of Pr dopant content. The position of $3d_{5/2}$ peak with binding energy of 932.5 eV is associated with +3 oxidation state of praseodymium in perovskite structure while the visible peak at 934.3 eV corresponds to the Pr^{4+} cations. These results are confirmed with previous studies by other research group investigating the association of praseodymium on a various oxidation states [25–27]. There are also an additional satellite peaks associated with the hybridization of valence orbitals and the effect of multiplet coupling, which makes the spectrum shape quite widen [26].

The all results are compared in Table 3. The performed measurements show that the presence of praseodymium dopant in the sample affects on valence state of titanium. In reduced samples, the ratio Pr^{3+} to Pr^{4+} is about 2:1. The study did not show the presence of praseodymium on the +2 oxidation state.

As been mentioned in the introduction section, although there are few papers about the Pr doped $SrTiO_3$ [21, 22, 28–31], it is still unclear what kind of Pr cation (Pr^{3+} or Pr^{4+}) incorporates in the Sr or Ti sublattice. The XPS measurement revealed the mixed valence state of Pr, where the fraction of Pr^{4+} cations of the used dopant concentration is relatively high. On the other hand, the stability of the doped perovskite cubic structure can be easily checked by the Goldschmidt factor calculation. In this work, we decided to check to tolerance factor for a sample with a 30 mol% of Pr in the structure. The calculations were performed for a previously reported ionic radius of Pr^{3+} (1.13 Å) and Pr^{4+} (0.96 Å) for a CN = 8 [32]. Under the first assumption, where the Pr fully incorporates into the Sr lattice (65% Pr^{3+} and 35% Pr^{4+}), the tolerance factor is equal to 1.044 what indicates the tetragonal distortion of the structure. This result contradicts with a XRD results showed in Fig. 1. The second possible and checked situation is that the tetravalent Pr cation substituted the Ti sublattice and trivalent Pr cation incorporates into the Sr lattice. In this case the tolerance factor was equal to 0.968. This is a characteristic value for a stable perovskite structure, which can be visible in a XRD pattern for 30% Pr sample in Fig. 1. The third possible situation is when a both Pr^{3+} and Pr^{4+} cation substitutes a titanium sublattice. The tolerance factor calculated for this assumption is 0.94, what indicates a cubic structure. According to the XRD measurements it can be stated, that this situation can be also possible. However, the XPS studies shown that the concentration of Ti^{3+} cations increases with a Pr^{3+} concentration in sample. Thus, in reference to the defect

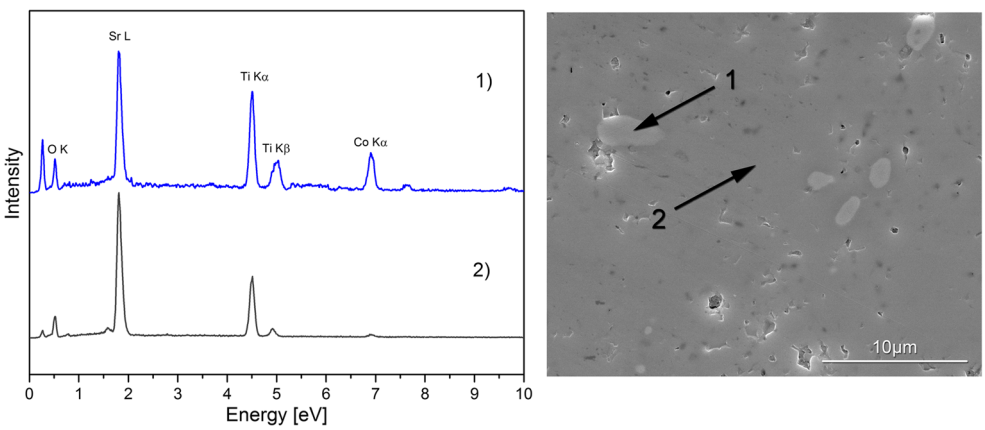

Fig. 5 EDX measurement with the SEM image of the marked locations of research polished cross-section surface of 0%Pr sample

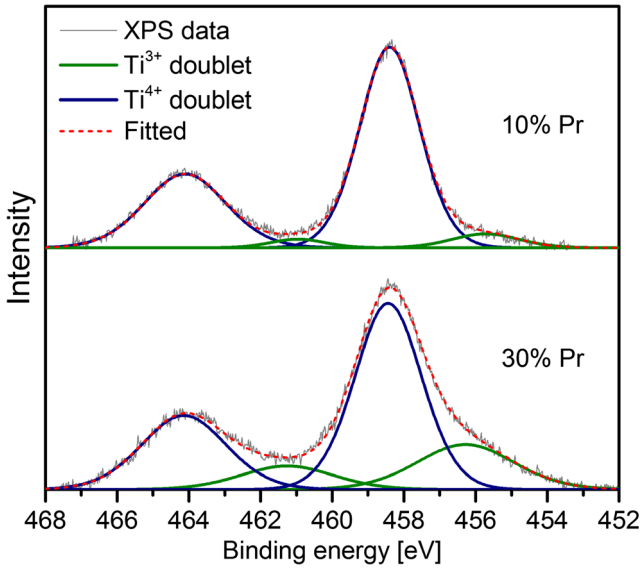

Fig. 6 Ti 2p core-level region for reduced Pr30% and Pr10% samples

chemistry shown in Eqs.2 and 6, it indicates, that a Pr^{3+} is a donor dopant only into the Sr^{2+} sublattice.

In order to check the mechanical stability of the samples, the dilatometry technique measurements were conducted to determine the thermal expansion coefficient of synthesized materials. The results are shown in Fig. 8. As can be seen, during heating in argon atmosphere, above 300 °C a significant change in sample relative length was observed. Those analyzed materials were sintered under hydrogen atmosphere (10^{-23} atm. pO_2). Therefore, during dilatometric measurements under much higher oxygen partial pressure (argon atmosphere - 10^{-6} atm. pO_2) samples were partially oxidized. That process is visible during heating of samples. Moreover, the initial temperature where the rapid elongation process was

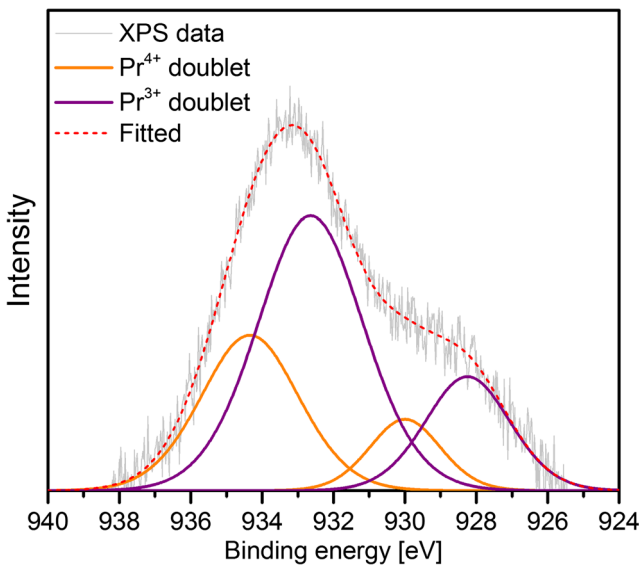

Fig. 7 $Pr3d_{5/2}$ deconvoluted XPS spectra for reduced $Sr_{0.7}Pr_{0.3}Ti_{0.93}Co_{0.07}O_{3-\delta}$ sample

Table 3 The valence states of praseodymium and titanium in studied materials

Sample	Pr $3d_{5/2}$ (± 3%)		Ti 2p (± 3%)	
	Pr^{3+}	Pr^{4+}	Ti^{3+}	Ti^{4+}
0% Pr	–	–	–	100%
10% Pr	69%	31%	7%	93%
20% Pr	72%	28%	13%	87%
30% Pr	65%	35%	19%	81%

begun decreases with an increasing of Pr concentration in the sample. It might seem that the oxidation of the sample should decrease unit cell parameters because of the incorporation of oxygen into the oxygen vacancies and in consequence, change of Pr and Ti valance state, as was previously reported *i.a.* by Thampi et al. [33]. An opposite behavior, observed in this work, may be related to the hypothesis, that praseodymium dopant can partially substitute both Sr^{2+} and Ti^{4+}/Ti^{3+} sublattice (see Eq.4). Changing of the oxidation state of praseodymium cations may cause a diffusion of Pr atoms from strontium to titanium sublattice. In such a case, changes of TEC and other structural parameters observed during the redox cycles (oxidation/reduction) may be more complex. In order to explain it in details, more advanced structural analysis is necessary.

During the measurement, a new thermodynamic equilibrium is established, which confirms the further linear increase of thermal expansion coefficient above 600 °C. The space between the straight lines represents different samples illustrates how much the sample length has changed after the oxidation process. The TEC values of all materials after the full oxidation were determined by fitting a linear dependence with the results obtained during a cooling step.

The obtained TEC values for all tested materials were added to the Fig. 8. It can be noticed, that the obtained TEC values were quite similar in all materials both in reduced and oxidized form and was about $1.17–1.26 \cdot 10^{-5}$ K^{-1}. These TEC values were very close to the YSZ electrolyte value (approximately $1.31 \cdot 10^{-5}$ K^{-1} [34]). Thus, these materials can be considered as an electrodes in electrochemical SOFC/SOEC devices.

4.2 Electrical properties

The electrical conductivity level is a crucial parameter in case of eventual application of the materials in electrochemical devices. The investigations of the electrical conductivity of the synthesized compounds using the DC- four point method were performed. For comparison the electrical conductivity in different atmospheres, each of samples sintered in H_2 was measured at hydrogen atmosphere and then oxidized in

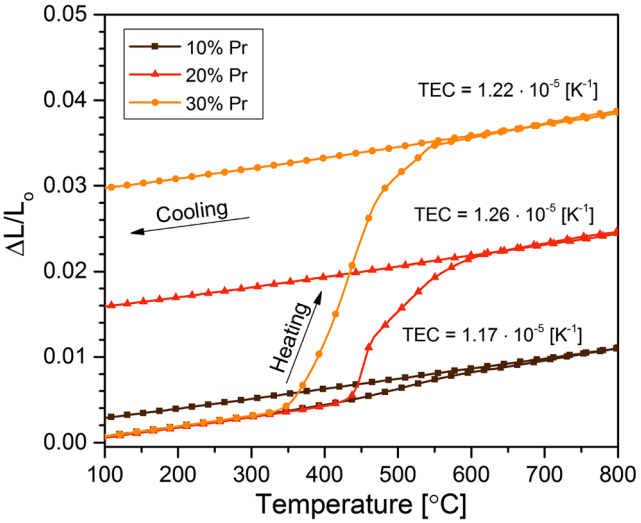

Fig. 8 Thermal expansion coefficient for samples sintered in hydrogen and then oxidized in situ during dilatometric measurement

air atmosphere for measure the behavior in air conditions. It has to be noticed, that the measurements of the temperature dependence σ(T) include a porosity Bruggeman correction (Eq.7):

$$\sigma_{mat} = \sigma_{meas}\left(1-\frac{p}{100}\right)^{-3/2} \quad (7)$$

where σ_{mat} is a total conductivity of dense material, σ_{meas} denotes measured conductivity of a porous sample and p is a total porosity value [35]. The temperature dependence of total electrical conductivity in a function of 1000 T^{-1} for reduced samples is presented in Fig. 9. As can be noticed, regardless of the Pr donor dopant content, the total conductivity increased with increasing temperature, what may indicate the thermally active conduction mechanism characteristic in the doped $SrTiO_3$ materials. The total conductivity values increase with a Pr dopant concentration it may be explained by the increase of the Ti^{3+} (This increase was also proved by XPS studies – see Table 3.) These observations are in agreement with a defect chemistry model shown in Eq.5. and suggest that praseodymium 3+ incorporates mainly into the Sr sublattice. The measured electrical conductivities at 800 °C were $3{\cdot}10^{-2}$; 2.5; 6.9 and 23.7 $S{\cdot}cm^{-1}$ for samples with 0, 10, 20 and 30 mol% of Pr in the structure, respectively. It is important to note that all of doped materials have reached the required conductivity level for SOEC electrodes (> 1 Scm^{-1}) at 650 °C for 10 mol% content of Pr in the structure, at 550 °C for 20 mol% of Pr, and at 300 °C for sample with 30 mol% amount of Pr. The $SrTiO_3$ sample only acceptor doped by Co exhibits quite low conductivity, around 2 orders of magnitude lower than these co-doped by Pr and Co. This is an expected behavior in reference to the defect chemistry of acceptor-doped $SrTiO_3$ at low pO_2 regimes. The same behavior was previously observed in the literature [20, 36].

In order to check the influence of the sintering atmosphere on the electrical properties, the all four analyzed samples previously sintered at H_2 were oxidized in situ during a DC 4-wire experiment. The measurement was performed after full oxidation of the samples. The temperature dependence σ(T) of total conductivity vs 1000 T^{-1} for oxidized samples is presented in Fig. 10. As can be seen, the conductivity level of analyzed samples suddenly decreases in air atmosphere even 4–5 orders of magnitude. This behavior is related to the oxidation

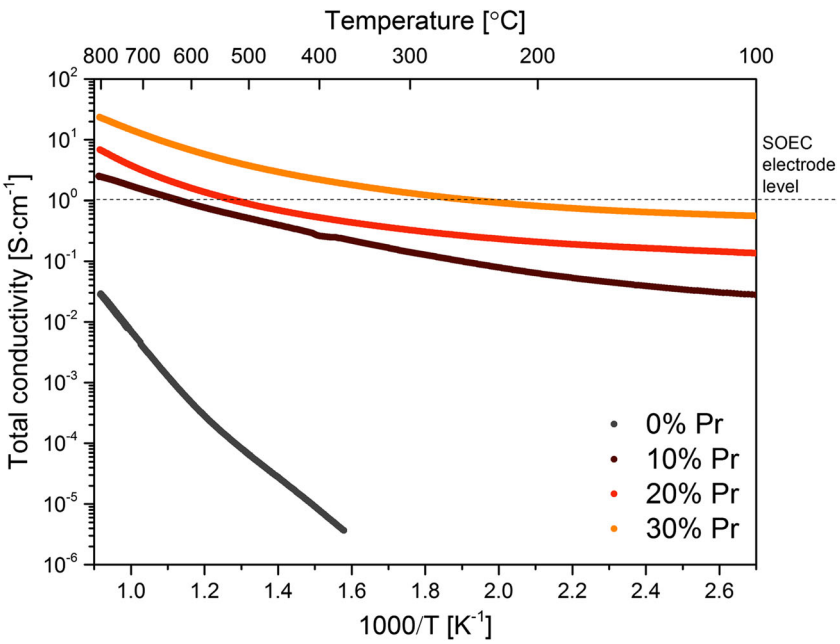

Fig. 9 The temperature dependence of the total electrical conductivity in hydrogen atmosphere $Sr_{1-x}Pr_xTi_{0.93}Co_{0.07}O_3$ samples after synthesis in H_2

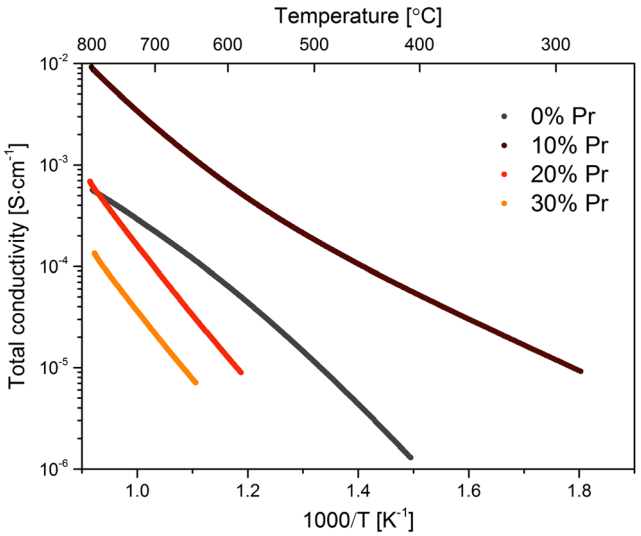

Fig. 10 The temperature dependence of the total electrical conductivity in oxygen atmosphere $Sr_{1-x}Pr_xTi_{0.93}Co_{0.07}O_3$ samples oxidized in-situ during measurements

process, where the concentration of conductive Ti^{3+} cations decreases. It was also observed, that a substitution of Pr in the structure results in a lower conductivity – the σ value decreases with an increase of a praseodymium donor concentration. This is a consistent result with defect chemistry of Pr, Co – co doped $SrTiO_3$ analyzed at high pO_2 regimes (Eq.4) under the assumption, that a triavalent praseodymium cation (Pr^{3+}) substitutes a strontium sublattice.

5 Summary and conclusions

A samples of $Sr_{1-x}Pr_xTi_{0.93}Co_{0.07}O_3$ (x = 0–0.3) were successfully synthesized at high temperature in H_2 atmosphere by a conventional solid state synthesis method. According to the XRD results, in all obtained samples the cubic perovskite $SrTiO_3$ phase was observed. XPS studies have shown that a praseodymium exist on mixed +3 and + 4 oxidation state. These studies and also the observed change in the lattice parameter as well as the analysis of changes in electrical conductivity allow to suppose that the praseodymium is incorporated both into the titanium and strontium sublattice. In the Ti sublattice tetravalent praseodymium is an isovalent dopant, however its presence influences on partial reduction of Ti^{4+} to Ti^{3+} what should effects on the conductivity of the material. On the other hand, a trivalent praseodymium substitutes strontium which makes it an acceptor dopant.

Obtained materials with co-doped by Pr and Co has favorable microstructure also the thermal expansion coefficient is close to the YSZ electrolyte value. The electrical conductivity in pure hydrogen is relatively high. Minimum requirement in SOFC/SOEC electrodes (conductivity>1 S cm^{-1}) was reached 650 °C for 10 mol% content of Pr in the structure, at 550 °C for 20 mol% of Pr, and at 300 °C for sample with 30 mol% amount of Pr. All this features provide the basis for further work on the development of this material as novel fuel electrode materials for SOFC/SOEC cells.

To summarize, the aim of this work was to investigate the stability of a $Sr_{1-x}Pr_xTi_{0.93}Co_{0.07}O_{3-\delta}$ perovskite materials in a wide pO_2 range. The observed significant conductivity changes at high pO2 (see Fig. 10) are related to the structural changes, thus further analysis including deep Rietveld, XANES or neutron diffraction should be done. Moreover, the different synthesis route may have a great impact to the properties of $Sr_{1-x}Pr_xTi_{0.93}Co_{0.07}O_{3-\delta}$ system. Thus, the sintering of the materials at oxidizing atmosphere and further reduction as a separate synthesis stage may improve the stability.

Acknowledgements This work is supported by project founded by National Science Centre Poland based on decision DEC-2015/19/D/ST8/02783.

References

1. S. Chen, K. Xie, J. Power Sources **274**, 718–729 (2015)
2. S.D. Ebbesen, C. Graves, A. Hauch, S.H. Jensen, M. Mogensen, J. Electrochem. Soc. **157**(10), 1419–1429 (2010)
3. Z. Jiao, N. Takagi, N. Shikazono, N. Kasagi, J. Power Sources **196**(3), 1019–1029 (2011)
4. Q. Qin, G. Wu, Electrochim. Acta **127**, 215–227 (2014)
5. B. Ge, J. Ma, Electrochim. Acta **151**, 437–446 (2015)
6. C. Zener, Phys. Rev. **82**(3), 403–405 (1951)
7. L.-W. Tai, M.M. Nasrallah, H.U. Anderson, D.M. Sparlin, S.R. Sehlin, Solid State Ionics **76**(3-4), 259–271 (1995)
8. K. Müller, H. Burkard, Phys. Rev. B **19**(7), 3593–3602 (1979)
9. M.C. Verbraeken, T. Ramos, K. Agersted, Q. Ma, C.D. Savaniu, B.R. Sudireddy, J.T.S. Irvine, P. Holtappels, F. Tietz, RSC Adv. **5**(2), 1168–1180 (2015)
10. S. Hui, A. Petric, J. Electrochem. Soc. **149**(1), J1–J10 (2002)
11. T. Ishihara, Springer Science Business Media, LLC (2009) 1-6; p. 168–169
12. S. Hui, A. Petric, J. Eur. Ceram. Soc. **22**(9-10), 1673–1681 (2002)
13. Q. Ma, F. Tietz, A. Leonide, E. Ivers-Tiffée, J. Power Sources **196**(17), 7308–7312 (2011)
14. R. Moos, W. Menesklou, H.-J. Schreiner, K.H. Härdtl, Sensors Actuators B Chem. **67**(1-2), 178–183 (2000)
15. J. Exner, M. Schubert, D. Hanft, T. Stöcker, P. Fuierer, R. Moos, Sensors Actuators B Chem. **230**, 427–433 (2016)
16. S. Suthirakun, G. Xiao, S.C. Ammal, F. Chen, H.-C. zur Loye, A. Heyden, J. Power Sources **245**, 875–885 (2014)
17. S. Suthirakun, S.C. Ammal, G. Xiao, F. Chen, F.K. Huang, H.-C. zur Loye, A. Heyden, Solid State Ionics **228**, 37–45 (2012)
18. X. Li, H. Zhao, N. Xu, X. Zhou, C. Zhang, N. Chen, Int. J. Hydrog. Energy **34**(15), 6407–6414 (2009)

19. X. Li, H. Zhao, F. Gao, Z. Zhu, N. Chen, W. Shen, Solid State Ionics **178**, 1588–1592 (2008)
20. A. Yaremchenko, J. Macías, J. Frade, V Iberian Symposium on Hydrogen, Fuel Cells and Advanced Batteries. Tenerife, España, July 05-08 (2015) p. 174–177
21. K. Park, J. Kim, J. Bae, Solid State Ionics **272**, 45–52 (2015)
22. D.P. Fagg, V.V. Kharton, A.V. Kovalevsky, A.P. Viskup, E.N. Naumovich, J.R. Frade, J. Eur. Ceram. Soc. **21**(10-11), 1831–1835 (2001)
23. G.S. Lewis, A. Atkinson, B.C.H. Steele, J. Mater. Sci. Lett. **20**(12), 1155–1157 (2001)
24. R.P. Vasquez, Surf. Sci. Spectra **1**, 129–135 (1992)
25. C.D. Wagner, W.M Riggs, L.E Davis, J.F. Moulder, *Handbook of X-ray Photoelectron Spectroscopy.* (Perkin-Elmer, 1978)
26. H. Ogasawara, A. Kotani, R. Potze, G.A. Sawatzky, B.T. Thole, Phys. Rev. B **44**(11), 5465–5469 (1991)
27. S. Lutkehoff, M. Neumann, A. Slebarski, Phys. Rev. B **52**(19), 13808–13811 (1995)
28. L. Zhang, X. Zhua, Z. Caoa, Electrochim. Acta **232**, 542–549 (2017)
29. A. Dehkordi, S. Bhattacharya, T. Darroudi, H. Alshareef, T. Tritt, J. Appl. Phys. **117**(5), 055102 (2015). https://doi.org/10.1063/1.4905417
30. A.A. Yaremchenko, S.G. Patrício, J.R. Frade, J. Power Sources **245**, 557–569 (2014)
31. I.A. Sluchinskaya, A.I. Lebedev, A. Erko, J. Appl. Phys. **112**(2), 024103 (2012)
32. R.D. Shannon, Acta Cryst **A32**, 751–767 (1976)
33. V. Thampi, P.R. Padala, A.N. Radhakrishnan, New J. Chem. **39**(2), 1469–1476 (2015)
34. S. Nath, I. Manna, A.K. Jha, S.C. Sharma, S.K. Pratihar, J.D. Majumdar, Ceram. Int. **43**(14), 11204–11217 (2017)
35. D.A.G. Bruggeman, Ann. Phys. **416**(7), 636–664 (1935)
36. A. Rothschild, M. Wolfgang, H.L. Tuller, E. Ivers-Tiffée, Chem. Mater. **18**(16), 3651–3659 (2006)